RESEARCH ARTICLE



Wiley

A hydrologic signature approach to analysing wildfire impacts on overland flow

L. A. Bolotin 🕒 | H. McMillan 🕩

Department of Geography, San Diego State University, San Diego, California, USA

Correspondence

H. McMillan, Department of Geography, San Diego State University, San Diego, CA, USA. Email: hmcmillan@sdsu.edu

Funding information

National Science Foundation, Grant/Award Number: 2124923

Abstract

Post-fire flooding and debris flows are often triggered by increased overland flow resulting from wildfire impacts on soil infiltration capacity and surface roughness. Increasing wildfire activity and intensification of precipitation with climate change make improving understanding of post-fire overland flow a particularly pertinent task. Hydrologic signatures, which are metrics that summarize the hydrologic regime of watersheds using rainfall and runoff time series, can be calculated for large samples of watersheds relatively easily to understand post-fire hydrologic processes. We demonstrate that signatures designed specifically for overland flow reflect changes to overland flow processes with wildfire that align with previous case studies on burned watersheds. For example, signatures suggest increases in infiltration-excess overland flow and decrease in saturationexcess overland flow in the first and second years after wildfire in the majority of watersheds examined. We show that climate, watershed and wildfire attributes can predict either post-fire signatures of overland flow or changes in signature values with wildfire using machine learning. Normalized difference vegetation index (NDVI), air temperature, amount of developed/undeveloped land, soil thickness and clay content were the most used predictors by well-performing machine learning models. Signatures of overland flow provide a streamlined approach for characterizing and understanding post-fire overland flow, which is beneficial for watershed managers who must rapidly assess and mitigate the risk of post-fire hydrologic hazards after wildfire occurs.

KEYWORDS

debris flows, flooding, hydrologic signatures, machine learning, overland flow, post-fire

INTRODUCTION 1

Wildfires followed by extreme rainfall can cause flooding and debris flows such as the deadly 2018 debris flows in Montecito, California, United States (Kean et al., 2019). These compound hazards are an increasing risk as extreme precipitation and wildfire intensify with a changing climate (Abatzoglou & Williams, 2016; AghaKouchak et al., 2020; Yin et al., 2018). Post-fire flooding is primarily caused by overland flow, in which surface runoff occurs due to rainfall intensities that exceed soil infiltration capacity (infiltration-excess [IE] overland flow (Horton, 1933)) or rainfall occurring over an already saturated soil profile (saturation-excess overland flow (Dunne & Black, 1970)). Wildfire increases watershed susceptibility to overland flow through processes including increasing soil hydrophobicity (DeBano, 2000; DeBano & Krammes, 1966; Doerr et al., 2000), reducing infiltration capacity (Ebel & Moody, 2017) and removal of biomass that previously intercepted precipitation or provided water storage and surface roughness in the litter layer (Leighton-Boyce et al., 2007).

This is an open access article under the terms of the Creative Commons Attribution License, which permits use, distribution and reproduction in any medium, provided the original work is properly cited.

© 2024 The Author(s). Hydrological Processes published by John Wiley & Sons Ltd.

These impacts on soils can promote IE overland flow and associated debris flows in burned watersheds (Rengers et al., 2020). Additionally, runoff from saturated soils can cause post-fire hazards via shallow landslides (DeBano, 2000; Wall et al., 2020).

The impact of wildfire on surface runoff depends on watershed characteristics such as dominant vegetation type and antecedent moisture levels (Dick et al., 1997; Stoof et al., 2012). Improving the understanding of the process mechanisms, spatial patterns and drivers of post-fire overland flow would be of significant societal benefit given precipitation extremes and occurrence and severity of wildfires are expected to increase with climate change (Wilder et al., 2021; Yin et al., 2018). When intense precipitation falls on recently burned watersheds, runoff-generated debris flows and flooding, which pollutes freshwater resources and threaten life and property, become a significant risk (Basso et al., 2020; Kean et al., 2019; Rengers et al., 2020). This risk is greatest during the first two years after wildfire (Shakesby & Doerr, 2006; Stoof et al., 2012). However, hydrologic recovery from wildfire can take anywhere from a few years to several decades and varies with watershed characteristics (Wagenbrenner et al., 2021).

Large-sample studies have developed our understanding of the spatial distribution of dominant runoff generation mechanisms across the United States, including identifying catchments dominated by IE versus saturation-excess overland flow (Buchanan et al., 2018; Wu et al., 2021). However, wildfire can shift these dominant runoff generation mechanisms from one process to another, such as from saturation-excess to IE dominated (Chen et al., 2013). Changes in dominant processes warrant adapted management practices to mitigate the time-sensitive impacts of post-fire flooding or debris flows (Rengers et al., 2019) and are thus critical to understanding at broad spatial scales in wildfire-prone regions. In this study, we investigated wildfire impacts on dominant overland flow processes across a dataset of 39 fire-impacted watersheds.

We used hydrologic signatures to quantify changes in the occurrence and prevalence of overland flow processes. Hydrologic signatures are indices calculated from streamflow and occasionally precipitation time series that quantify aspects of the hydrologic regime of a catchment (Gupta et al., 2008; McMillan, 2021). Signatures can be used as objective functions in hydrologic models (Shafii & Tolson, 2015) or can inform decisions about model structure (David et al., 2022) to improve similarity between simulated and observed runoff patterns. Hydrologic signatures facilitate further understanding of hydrologic processes when carefully selected, as different signatures represent the occurrence and/or magnitude of specific processes including evapotranspiration, baseflow and overland flow (McMillan, 2020). Signatures of overland flow have promoted our understanding of this process outside of post-fire contexts (McMillan, 2020; Wu et al., 2021). Signatures not specific to overland flow such as runoff ratio have been applied to understand the timing of hydrologic recovery after wildfire (Hampton & Basu, 2022; Wagenbrenner et al., 2021; Wilder et al., 2021). However, overland flow signatures have not previously been used to evaluate post-fire hydrologic processes. Leveraging these process-specific signatures provides a method for analysing wildfire impacts on potentially flood-inducing runoff generation without requiring the time-consuming calibration and running of hydrologic models.

The limited data requirements of hydrologic signatures allow them to be calculated and automated for many watersheds, which promotes the feasibility of large-sample studies. The increasing availability of large-sample hydrometeorological datasets has already facilitated several continental-scale studies identifying regional patterns of hydrologic processes and providing deeper insights into the functionality of hydrologic signatures themselves (Addor et al., 2018; McMillan et al., 2022; Wu et al., 2021). Catchment attributes paired to streamflow sites (Addor et al., 2017; Wieczorek et al., 2018) can be used to predict hydrologic signatures and further promote process understanding via machine learning (ML) approaches. ML models provide predictor variable importance rankings, making them useful for inferring which attribute(s) contribute most to the accuracy of the streamflow signature prediction and may thus be drivers or products of different processes (Addor et al., 2018; Jehn et al., 2020; Wu et al., 2021).

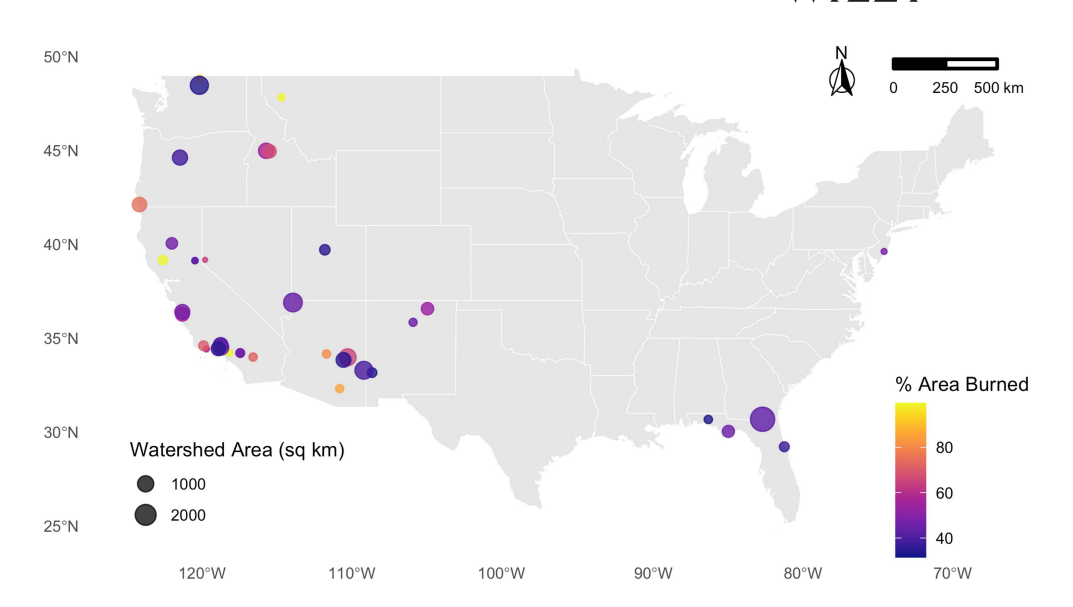
While several post-fire runoff studies acknowledge the influence of static catchment attributes (e.g. soil type, underlying geology, topography, etc.) on the changes between pre- and post-fire runoff processes, detailed analysis of which attributes exert the greatest influence has often been out of the scope of the research (Hampton & Basu, 2022; Kean & Staley, 2021). Previous comparisons of various regression methods using wildfire and watershed attributes to predict non-overland flow-specific hydrologic signatures have yielded low correlation coefficients and/or contradictory findings (Saxe et al., 2018). Focusing on one process such as overland flow could elucidate the links between these attributes and post-fire hydrologic response. Predicting changes in signatures of overland flow and consequently identifying the attributes of fires, climate and watersheds themselves that play the largest role in determining postfire surface runoff behaviour can aid in post-fire watershed management across the United States, especially if regional patterns emerge from the analysis.

Here, we leverage hydrologic signatures specific to overland flow and use large-sample hydrometeorological datasets to investigate (1) whether signatures of overland flow change significantly to reflect shifts in runoff generation mechanisms after wildfire, (2) the timescale of wildfire impacts on signatures of overland flow and (3) the most important predictors of post-fire overland flow signatures.

2 | DATA AND METHODS

2.1 | Watershed selection

To improve the generalized process understanding of post-fire overland flow, we analysed 39 watersheds with areas ranging from approximately 13 to 2927 km² that have been significantly burned by wildfire or prescribed burns in the United States (Figure 1). A summary of watershed information is provided in the Supplemental Information. We selected watersheds from the Geospatial Attributes of Gages for Evaluating Streamflow (GAGES-II) dataset (Falcone, 2011). We excluded watersheds with more than one major dam upstream to minimize confounding drivers of hydrologic response. We required



that watersheds had at least 20% of their area forested, assuming forested landscapes experience particularly large hydrologic impacts from wildfire (Hampton & Basu, 2022). To ensure adequate data to characterize pre- and post-fire runoff conditions, we required that watersheds have at least 10 years of streamflow and precipitation data available both pre- and post-fire. We excluded sites where more than 10% of this 20-year time series was missing. Despite the large number of watersheds in the GAGES-II dataset meeting the burned and forested area requirements (109), these strict requirements for streamflow data eliminated 64% of eligible sites from the study, with 39 sites meeting all requirements. Previous studies also faced challenges of limited data availability for either the pre- or post-fire period, if not both (see the review by Wagenbrenner et al., 2021).

To calculate the proportional burned area of each watershed, we intersected shapefiles of burn perimeters from the Monitoring Trends in Burn Severity (MTBS) dataset (Eidenshink et al., 2007) and watershed boundaries from GAGES-II. The MTBS dataset provides shapefiles for wildfires and prescribed burns 1000 acres or larger between 1984 and 2020. We filtered the watersheds for those where at least 30% of the watershed was burned within one fire season, including from multiple fire events. We assumed fire seasons were contained within calendar years, given that the majority of fire ignition dates occurred in the summer months (Figure S1). Since MTBS only includes fires of 1000 acres or larger, some smaller fire-impacted watersheds were not identified for this study and the impact of fires <1000 acres in the selected catchments was not considered. If an eligible watershed had 30% or more of its area burned multiple times within 10 years of each other, it was excluded, as reburns could confound the hydrological impacts of the initial fire.

2.2 | Hydrometeorological data

To analyse pre- and post-fire overland flow processes using hydrologic signatures, we used streamflow data from the National Water

Information System, accessed through the dataRetrieval package in R (De Cicco et al., 2018). We used precipitation data from the North American Land Data Assimilation System (NLDAS) (Xia et al., 2012). We chose NLDAS for its hourly temporal resolution with data beginning in 1979, making it possible to access rainfall data for a large sample of watersheds from a single source. We summed hourly rainfall data into daily values for sites where only daily streamflow data was available. Area-weighted NLDAS precipitation data was obtained using wrfhvdroSubsetter (github.com/mikejohnson51/wrfhydroSubsetter). While daily streamflow data can be used successfully for signature calculation, the short, intense precipitation events that typically cause post-fire hydrologic hazards call for a finer temporal scale for the data when available (e.g. hourly or sub-hourly rather than daily) (Kean et al., 2011). This may be particularly important for smaller watersheds with shorter times of concentration (Beven, 2020). Comparisons of hourly and daily overland flow signature values and their agreement with field observations suggest that hourly data is ideal for calculating overland flow signatures McMillan et al. (2022); therefore, we prioritized using hourly data in any watershed where it was available but maintained sites with only daily data available. We expect that the robustness of signature values in smaller watersheds where only daily data was available will be impacted the most given that smaller watersheds have shorter times of concentration and are more dominated by hillslope processes, which may be obscured in daily data (Robinson et al., 1995).

2.3 | Hydrologic signatures

We calculated four hydrologic signatures related to the prevalence of IE and saturation-excess (SE) overland flow to understand whether signatures of overland flow change significantly after fire in U.S. watersheds. We calculated the IE Regression and SE Regression signatures, representing prevalence of IE and SE overland flow, respectively, using the Toolbox for Streamflow Signatures in

Hydrology (TOSSH) in MATLAB (Gnann et al., 2021) (https://github.com/TOSSHtoolbox/TOSSH). These signatures were originally developed by Estrany et al. (2010) to differentiate IE and SE runoff mechanisms for agricultural areas in Mediterranean climate regions. To calculate the signatures, we used stepwise regression to fit coefficients a, b in Equations 1 and 2 that relate peak flow magnitude and total flow volume to normalized predictors X quantifying precipitation depth, antecedent precipitation and precipitation intensity. IE Regression is the mean of the coefficients of predictors related to intensity $(a_{4,5}, b_{4,5})$ and SE Regression is the mean of the coefficients of predictors related to precipitation depth and antecedent precipitation $(a_{1,2,3}, b_{1,2,3})$. In each case, the signature values range from -1 to 1, with higher values suggesting a prevalence of that mechanism.

$$Log Q_{Max} = a_1 X_1 + a_2 X_2 + a_3 X_3 + a_4 X_4 + a_5 X_5$$
 (1)

$$Log Q_{Ouickvol} = b_1 X_1 + b_2 X_2 + b_3 X_3 + b_4 X_4 + b_5 X_5$$
 (2)

where Q_{Max} is the maximum hourly event discharge (mm/h) and Q_{quickvol} is the total event quickflow volume (mm), X_1 is the total event precipitation (mm), X_2 and X_3 are the sum of 3-day and 5-day antecedent precipitation respectively (mm), X_4 is the mean event precipitation intensity (mm/h) and X_5 is the maximum event precipitation intensity (mm/h). X_{1-5} are normalized to have a mean of 0 and a standard deviation of 1 before use.

These signatures require initial processing to divide the rainfall and flow time series into individual storm events. TOSSH provides an event separation algorithm to characterize events into instances of >2 mm/h or 10 mm/day of rainfall. The events are separated by dry periods of at least 12 h and end 5 days after rainfall ceases. We maintained these default parameter values for the separation algorithm for all watersheds, though they are customizable. We filled missing values in the time series with NaN so they would be ignored by the TOSSH event separation algorithm. TOSSH also provides code for general streamflow indices like runoff ratio, which we calculated on an annual basis to identify and disqualify watersheds with potentially erroneous data or confounding impacts on hydrology. For example, site USGS-13239000 (North Fork Payette River at Mccall, ID), which had one major upstream dam control located immediately above the streamgage at a reservoir outlet, had a runoff ratio >1. This site was excluded from further analysis. TOSSH includes code for additional signatures to identify thresholds of precipitation required for generating overland flow, but in this study, we focus on signatures representing an overall prevalence of IE and SE overland flow.

The IE Correlation and SE Correlation signatures, like IE Regression and SE Regression, represent the prevalence of IE and SE overland flow, respectively. IE Correlation and SE Correlation were developed by Wu et al. (2021) to differentiate IE and SE runoff mechanisms for U.S. watersheds and were calculated using a modified version of code shared by the authors. IE Correlation is the Spearman correlation coefficient between event runoff ratio (total event quickflow volume (mm) divided by total event precipitation (mm)) and mean event precipitation intensity (mm/h). SE Correlation is the Spearman

correlation coefficient between event runoff ratio and total event precipitation (mm). The signature values range from -1 to 1, with higher values suggesting a prevalence of that runoff mechanism. The code was adapted to apply the TOSSH event separation algorithm, and therefore use the same guickflow events as those considered by the TOSSH signatures. The main difference between the event separation methods by Wu et al. (2021) and from TOSSH is that Wu et al. (2021) filtered for only the largest quickflow events. Using the same event separation algorithm for all signatures made them directly comparable. Calculating multiple signatures related to the same hydrologic processes and determining the similarities or differences in their values helps assess the robustness of the signatures for analysis of overland flow in a post-fire context. We calculated the signatures for the 10-year period prior to the ignition date of the first fire in the fire-year considered in each watershed, and for the 1-, 2-, 3-, 5- and 10-year periods after the ignition date of the last fire in that fire-year. We used the ignition date to mark both the end of the pre-fire period and the beginning of the post-fire period because 'fire-out' or containment dates were not available from MTBS for the majority of fires. In a few relatively arid watersheds, signatures for short timeperiods were calculated based on less than 10 quickflow events (7 and 5 sites for 1and 2-year post-fire signature values, respectively). We included these sites in the analysis given the limited eligible sites meeting the requirements for streamflow time series availability: however, it should be noted that signatures calculated on watersheds with so few events may not be as robust as signatures calculated for watersheds with more frequent quickflow events.

2.4 | Analysis of post-fire change in hydrologic signatures

To determine wildfire impacts on signature values, we calculated the absolute difference between signature values for the 10-year pre-fire period and the 1-, 2-, 3-, 5- and 10-year post-fire periods. For each signature, we determined the statistical significance of changes in the distribution of values across all sites between the 10-year pre-fire period and each post-fire period using the nonparametric Kolmogorov–Smirnov (K–S) test. The greatest vertical distance between the empirical cumulative distribution functions (CDFs) of pre- and post-fire signature values was quantified with the *D*-statistic, which has a value between 0 and 1. Higher values suggest a greater difference between the two distributions. We considered the two distributions to be statistically significantly different if the *p*-value was less than 0.05.

The signatures in Section 2.3 were calculated by McMillan et al. (2022) and Wu et al. (2021) for 546 and 432 watersheds, respectively, from the CAMELS dataset (Newman et al., 2015). We determined the percentile of the pre- and post-fire signature values for the 39 watersheds in this study (and thus the change in percentile with wildfire) in the distributions of values determined by McMillan et al. (2022) and Wu et al. (2021). This provided context for how significantly signature values changed from the pre- to post-fire period in comparison to typical values in U.S. watersheds.

TABLE 1 Summary of attribute data used in the relationship.	FABLE 1 Summary of attribute data used in the random forest.				
Attribute name	Citation or data source	Details			
Wildfire					
% Watershed burned	Calculated from MTBS and GAGES-II	-			
Difference-normalized Burn Ratio using the Thermal Band (dNBRT, proxy for Burn Severity)	Landsat 5 TM Collection 1 Tier 1 32-Day NBRT Composite; images courtesy of the U.S. Geological Survey	30-m spatial resolution; subtracted the minimum post-fire NBRT value from the averaged 10-year pre-fire NBRT value $NBRT = Near-Infrared - (Mid-Infrared \times Thermal)/Near-Infrared + (Mid-Infrared \times Thermal)$			
Soils					
Avg K_{sat} (saturated hydraulic conductivity)	Buchanan et al. (2018) (obtained directly from authors)	90-m spatial resolution			
Sand, silt, and clay content (%)	Wieczorek et al. (2018)	100-m spatial resolution resampled to 30-m			
Soil thickness					
Avg bulk density					
Organic matter (OM) content					
Topography					
Basin area	Wieczorek et al. (2018)	30-m digital elevation model			
Avg basin slope					
Avg stream slope					
Avg basin elevation					
Climate					
Avg aridity index	Calculated from NLDAS, Xia et al. (2012)	1/8° spatial resolution; averaged over the 10-years pre- and post-fire (20 years total)			
Avg precipitation	Wieczorek et al. (2018)	Averaged from 1971 to 2000			
Avg relative humidity		Averaged from 1961 to 1990			
Avg temperature		Averaged from 1971 to 2000			
Avg potential evapotranspiration		Averaged from 1971 to 2000			
Avg precipitation falling as snow (%)		Averaged from 1905 to 2002			
Land cover					
Land cover (developed land, open water, undeveloped land, forested land) (%)	Wieczorek et al. (2018)	30-m spatial resolution; Paired sites with data for the closest available pre-fire-year to the year of each fire onset year			
Pre-fire normalized difference vegetation index (NDVI)	Landsat 5 TM Collection 1 Tier 1 32-Day NDVI Composite and Landsat 8 Collection 1 Tier 1 32-Day NDVI Composite; images courtesy of the U.S. Geological Survey	30-m spatial resolution; averaged for the 10-year pre-fire period $\label{eq:NDVI} \mbox{NDVI} = \mbox{(Near-Infrared} - \mbox{Red)}/\mbox{(Near-Infrared} + \mbox{Red)}$			
Lithology					
Geologic K_2O , CaO, Fe_2O_3 , MgO, P_2O_5 , S, SiO_2 in surface or near-surface geology (%)	Wieczorek et al. (2018)	1-km spatial resolution			
Geologic strength					
Hydraulic conductivity					
Permeability					
Hydrology					
Avg depth to water table	Wieczorek et al. (2018)	-			
Stream density		-			

Note: Values represent the accumulated upstream area of each study site, and climate values are mean annual values. Avg = mean value.

In the highly variable Mediterranean climate of the southwestern U.S., drought or extreme precipitation events can explain much of the variation in hydrologic response after fire (Tomkins et al., 2008). Since watersheds in this study burned at various times between 1994 and 2011, we did not expect to see uniform changes in signature values due to differences in precipitation intensity or volume between the pre- and post-fire period. Nevertheless, we used a distribution comparison approach to evaluate potential differences between precipitation in the pre- and post-fire periods. We plotted the CDF of (1) maximum hourly precipitation intensity per day (mm/hour) and 2) total daily precipitation (mm/day) for each site, comparing the 10-year pre-fire with 2-year and 10-year post-fire distributions. We calculated the maximum difference between the two distributions for each site for both precipitation depth and intensity. This provided context as to whether changes may have been considerably impacted by precipitation anomalies rather than just by wildfire.

To understand how long wildfire impacts on overland flow signatures last, we compared the distributions of absolute change in hydrologic signature values between pre-fire and post-fire periods of varying lengths (1-, 2-, 3-, 5- and 10-years post-fire) in all watersheds. We observed which post-fire period(s) experienced the greatest changes compared to pre-fire conditions and whether the distributions recovered to pre-fire conditions during the 10-year post-fire period.

2.5 | Analysis of predictors of post-fire overland flow

We used an ML approach to investigate which wildfire, climate and physiographic catchment attributes were associated with changes in overland flow mechanisms with wildfire, as evidenced by hydrologic signatures. We created random forest (RF) regression models for each signature to predict (1) 10-year pre-fire signatures, (2) 10-year postfire signatures, (3) the absolute difference between 10-year pre-fire signatures and 10-year post-fire signatures, (4) 2-year post-fire signatures and (5) the absolute difference between 10-year pre-fire signatures and 2-year post-fire signatures. These target variables were chosen to determine whether these signatures can be predicted outside a post-fire context (hence the prediction of pre-fire values) and to provide insight into drivers of post-fire overland flow in the shortand long-term. We trained and ran the models using the randomForest package in R (Liaw & Wiener, 2002). The predictor variables and their sources are summarized in Table 1. We excluded predictors related to fire (percent of watershed burned and burn severity) from the models predicting pre-fire signature values since these predictors were not relevant to the unburned hydrologic condition. We recognize that large-domain gridded datasets as used here have varying and unknown uncertainty in their variables (Gupta et al., 2014). For example, as discussed by Beck et al. (2015), the limited quality and consistency of globally available datasets such as those for geology and soil characteristics may weaken relationships with streamflow characteristics, even where the processes controlled by these physical characteristics are well-accepted. In this study, we used predictor variables that are available across the United States from authoritative sources such as the U.S. Geological Survey (Wieczorek et al., 2018), although typically no uncertainty estimates are available for these variables. This method allows us to use a single data source for all watersheds in the study and allows our approach to be replicable for other large-sample studies.

To determine a reduced set of predictors and address multicollinearity, we identified all predictor pairs with a Spearman correlation coefficient of |0.85| or higher and selected one attribute from each pair of highly correlated attributes. For example, the average air temperature was highly correlated with the average potential evapotranspiration and percent of precipitation falling as snow, so only the average air temperature was retained. We used the caret package in R (Kuhn, 2008), to conduct recursive feature selection, identifying the most important predictors that can produce a simplified model with comparable performance to one with all the predictors. We excluded three watersheds from this portion of the analysis due to missing data for one or more predictors. Since we used one value per watershed for each model, sample sizes for the RFs were relatively small (n = 36) and results were dependent on the random sample of watersheds used to create a training dataset. Therefore, we ran an ensemble of 100 RF models with different initializations and randomly sampled training datasets for each signature.

Each model was trained on $^{3}/_{4}$ of the watersheds and tested on the remaining $^{1}/_{4}$. We evaluated model performance using R^{2} values to quantify the proportion of variance explained by the predictors. We used two methods to determine which predictor variables were most valuable in predicting overland flow signatures. First, we counted how many of the 100 RF ensemble members used each predictor variable for each signature. Then, we calculated an average value for the variable importance (increase in mean squared error or IncMSE, which is the loss in model accuracy if the values of a given predictor are permuted) for each predictor across all runs where that predictor was used. Both approaches provided rankings for which predictors were most important for estimating signatures of overland flow or changes to these signatures with wildfire.

3 | RESULTS

3.1 | Changes in hydrologic signatures with wildfire

We determined the absolute difference between pre- and post-fire signature values to understand changes with wildfire. The absolute differences between the signature values for 10 years pre-fire and the 2 and 10 years post-fire, respectively, are demonstrated in Figure 2. When considering changes between 10 years pre-fire and 2 years post-fire, 56% of sites experienced increases in IE Regression, 15% experienced no change and 28% experienced a decrease. For SE Regression, 82% of sites experienced decreases, one site experienced no change and 15% of sites experienced increases. Approximately half of the sites experienced increases in the IE Correlation and SE Correlation signatures (51% and 49%, respectively), while the remaining sites experienced decreases.

Patterns of change between 10 years pre-fire and 10 years post-fire were similar to those comparing the 10-year pre-fire and 2-year post-fire period, but the magnitude of changes was dampened in some watersheds. For IE Regression 10 years post-fire, 49% of sites

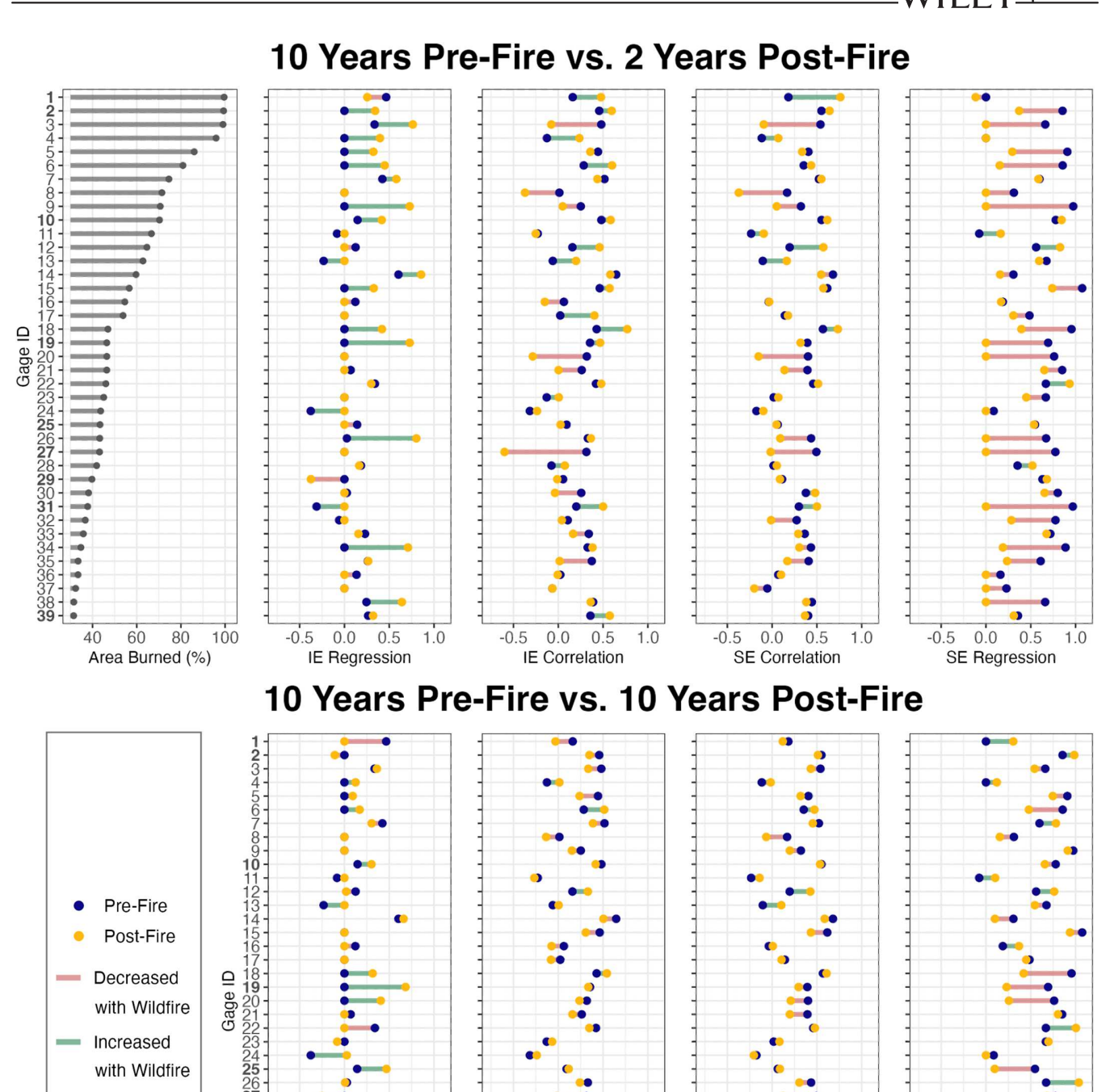


FIGURE 2 Plots showing absolute change between 10-year pre-fire and 2-year post-fire signature values (top row) and 10-year pre-fire and 10-year post-fire signature values (bottom row). The y-axis is ordered by the percentage of the watershed that was burned, with higher percentages at the top. Gage ID's in bold indicate sites with daily rather than hourly data.

0.0

IE Correlation

-0.5

0.5

1.0

experienced increases, 13% had no change and 38% experienced decreases. 62% of sites experienced decreases in SE Regression, 67% experienced decreases in SE Correlation, 69% experienced decreases

0.0 0.5

IE Regression

1.0

-0.5

in IE Correlation and the remainder of sites experienced increases in these signatures. In some cases, watersheds where signature values increased in the short-term post-fire period exhibited decreases when

1.0

0.0 0.5

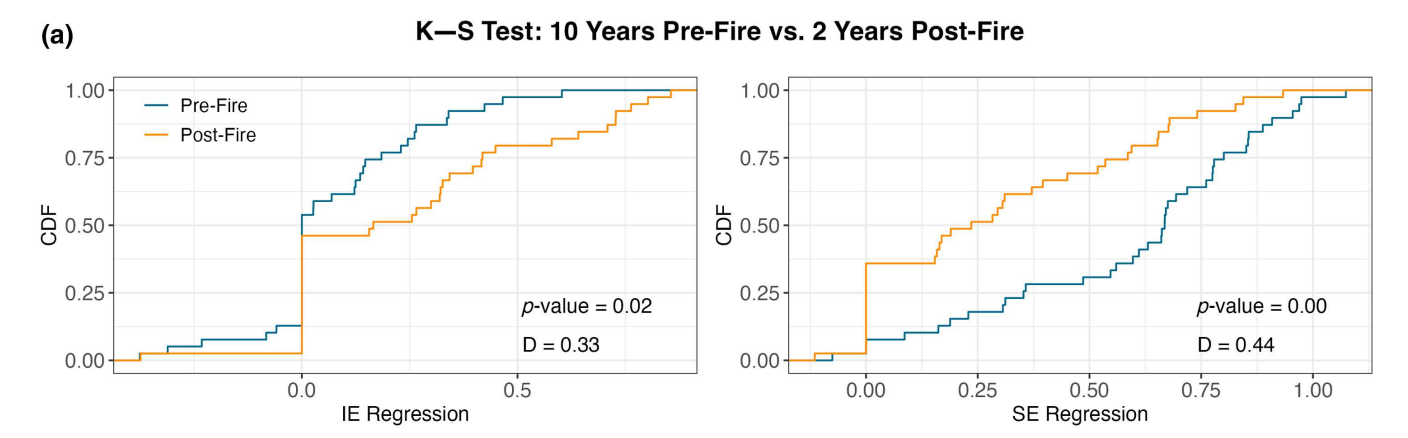
SE Correlation

0.0

SE Regression

-0.5

0.5



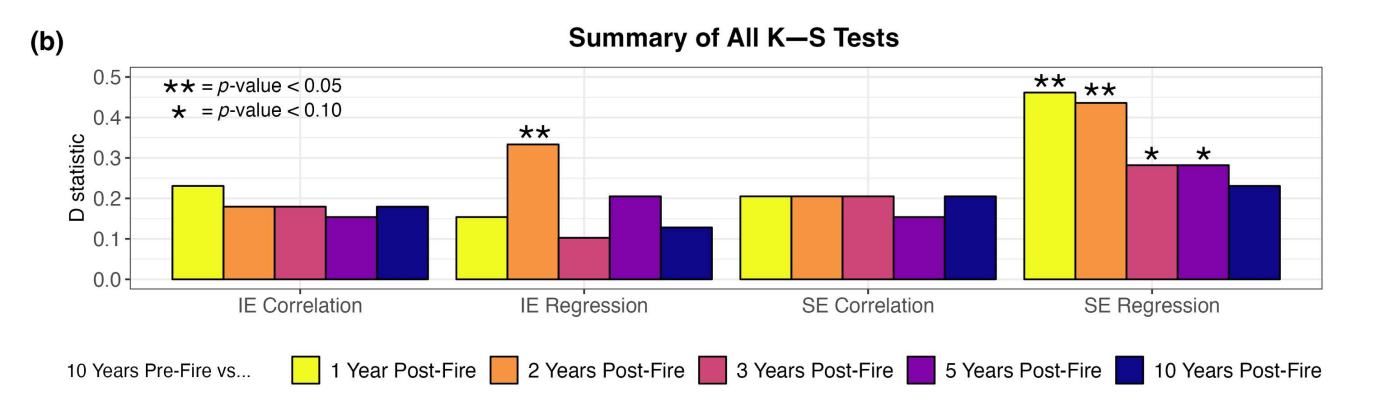


FIGURE 3 (a) Example Kolmogorov–Smirnov (K–S) test results showing statistically significant changes in a comparison of the distributions of 10-year pre-fire signatures with 2-year post-fire signatures across all sites. (b) Summary of all K–S test results.

a longer post-fire period was considered, or vice-versa (7 watersheds for IE Regression, 12 for SE Regression, 14 for IE Correlation and 12 for SE Correlation).

We expected to find higher values for signatures related to IE overland flow following wildfire, suggesting a higher prevalence of IE processes. Consequently, we expected to find lower values for SE processes (Liu et al., 2021). Changes in the IE Regression and SE Regression signatures followed these expected patterns, especially in the 2-year post-fire period with similar but less uniform trends in the 10-year post-fire period. The IE Correlation and SE Correlation signatures, which are also supposed to indicate the prevalence of infiltrationand saturation-excess processes, respectively, did not show the same clear trends 2 years post-fire but decreased for most watersheds in the 10-year post-fire period. In some cases, signatures designed for the same process (IE Regression and IE Correlation for IE overland flow, SE Regression and SE Correlation for SE overland flow) changed in contradictory directions in the same watershed for the same post-fire period.

We used K-S tests comparing the distributions of 10-year prefire signature values with distributions of 1-, 2-, 3-, 5- and 10-year post-fire values to assess the statistical significance of signature changes with wildfire. The K-S tests produced significant p-values (<0.05) for the pre-fire versus 1- and 2-year post-fire comparison of SE Regression and for the 2-year post-fire comparison of IE Regression (Figure 3). The tests produced D-statistics of 0.46 or lower.

While the K-S tests determined the statistical significance of changes in signature values with wildfire, comparison to signature values for watersheds across the United States provided context for the hydrological significance of changes. The change in percentile between 10-year pre-fire and 2-year post-fire signatures in a distribution of signature values for hundreds of U.S. watersheds is shown in Figure 4. For the IE Regression, SE Regression and IE Correlation signatures, the changes were often more considerable when contextualized in a national sample of values than when taken at face value. For example, a 0.32 absolute increase in IE Regression from 10 years pre-fire to 2 years post-fire at Gage ID 5 (USGS-09484000, Sabino Creek Near Tucson, AZ) was a change from the 8.6th percentile to the 85.3rd percentile in a national distribution of long-term signature values.

3.1.1 | Impacts of Precipitation Variability on Post-fire Signatures

We compared precipitation amount and intensity in the pre- and post-fire period to assess whether wildfire impacts on signatures of overland flow may be indiscernible from impacts of precipitation variability. The largest distance between the CDFs comparing 10-year pre- and post-fire precipitation was 0.18 for daily maximum

Change in Signature Value Percentile CONUS Distribution (10 Years Pre-Fire vs. 2 Years Post-Fire)

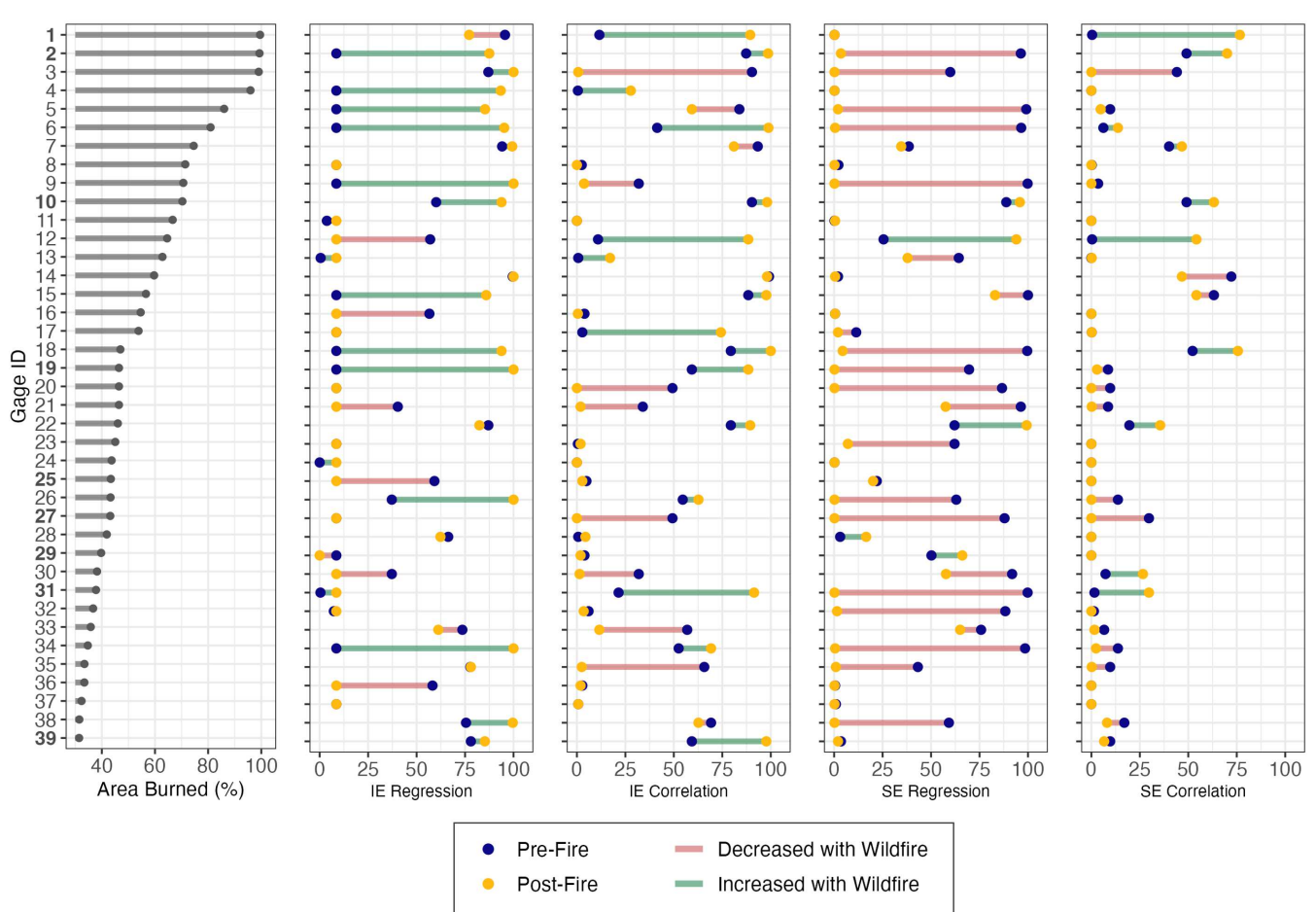


FIGURE 4 Dumbbell plots showing change in percentile (from a distribution of long-term signature values calculated for a large sample of watersheds in the contiguous U.S. (CONUS)) between 10-year pre-fire and 2-year post-fire signature values. The y-axis is ordered by the percentage of the watershed that was burned, with higher percentages at the top. Gage ID's in bold indicate sites with daily rather than hourly data.

precipitation intensity (mm/h) and 0.19 for total daily precipitation depth (mm/day) at Gage ID 6 (USGS-13310700, S. Fork Salmon River Near Krassel Ranger Station, Idaho). The largest distance between the CDFs comparing 10-year pre- and 2-year post-fire precipitation was 0.19 for daily maximum precipitation intensity (mm/h) and 0.18 for total daily precipitation depth (mm/day) at Gage ID 22 (USGS-11381500, Mill Creek Near Los Molinos, California). For context, the largest distance between two CDFs we could expect is 1. Graphical comparison of the CDFs demonstrates that even in these cases with the largest distances between curves, the distributions mostly overlap (Figure S2). The sections of the CDFs where the two distributions diverge most are not at the highest precipitation depths or intensities in the investigated watersheds. In most watersheds, we do not expect that a very small number of exceptionally high volume or intensity precipitation events in the pre- or post-fire period would substantially impact signature values. Potential exceptions to this would be instances where signatures are calculated for short time periods (1 or

2 years) in arid regions that have few rainfall-runoff events overall. Given the small differences observed between pre- and post-fire precipitation characteristics, we conclude that differences between pre- and post-fire signatures of overland flow can be attributed to wildfire impacts over climate variability.

3.2 | Timescales of recovery from wildfire impacts on overland flow signatures

We investigated changes in signatures of overland flow for various periods of time after wildfire to understand the timing of recovery of hydrologic processes after burning. When considering the change in signature values from 10 years pre-fire to 1, 2, 3, 5 and 10 years post-fire, changes were largest 1–2 years after wildfire. Regardless of whether signature values increased or decreased post-fire, they gradually recovered back to near pre-fire values throughout the 10-year

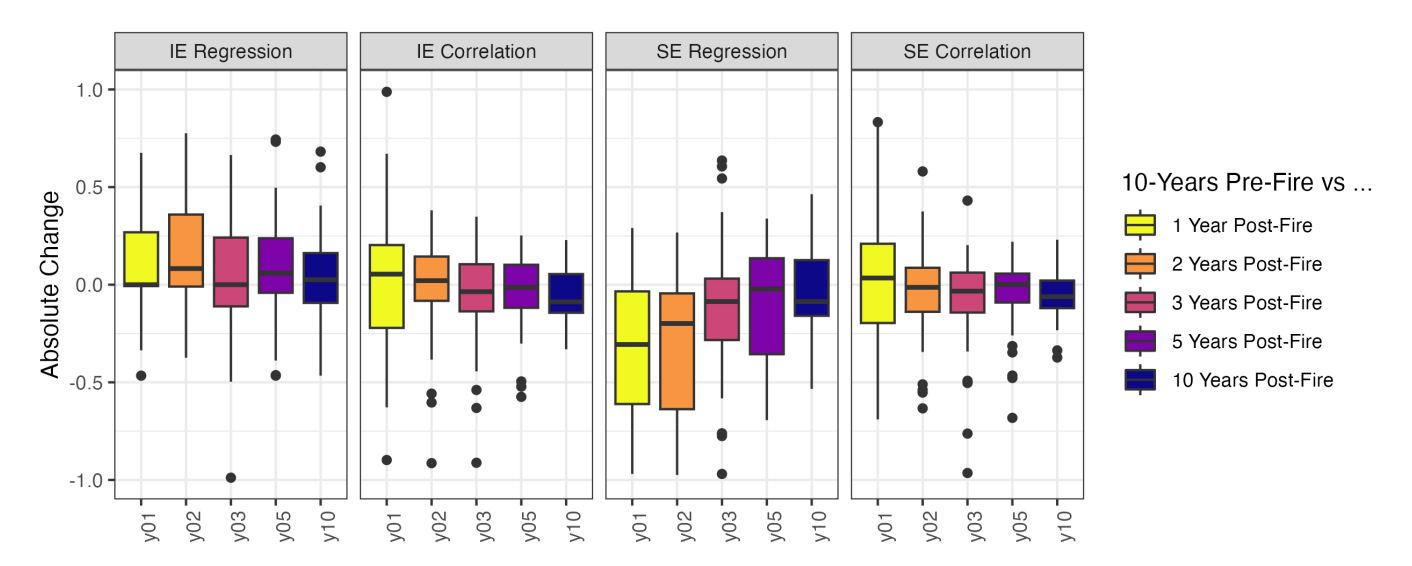


FIGURE 5 Boxplots showing the distribution of absolute change (post-fire value — pre-fire value) in signature values from 10 years pre-fire to 1, 2, 3, 5, and 10 years post-fire for the 39 study watersheds, where a value of 0 suggests no change, above 0 suggests an increase after wildfire, and below 0 suggests a decrease after wildfire.

post-fire period (Figure 5). IE Regression values were generally higher in the 1–2-year post-fire period, but the median absolute change value returns close to 0 (no change) when considering longer post-fire periods. The temporal patterns for IE Correlation generally follow that of IE Regression but reflect a wider range of absolute change values, especially in the negative direction (more sites showed decreases in this signature compared to IE Regression) one-year post-fire. The SE Regression signature shows an overall decrease with a wildfire that returns toward pre-fire conditions over time, whereas the SE Correlation shows an increase with a wildfire that decreases toward pre-fire levels over time.

3.3 | Predicting overland flow signatures post-fire

RF models successfully predicted either the change in signatures with wildfire or the pre- and post-fire signature values, depending on the signature. The R^2 values for the testing data set from the ensemble of 100 RF models for the IE Regression, IE Correlation, SE Correlation and SE Regression signatures are summarized in Table 2. Except for IE Regression, all pre-fire signatures were predicted with an ensemble median R² value of 0.45 and up to 0.59 for SE Correlation. Predictions of fire-impacted IE Regression and SE Regression had the highest performance in ensembles predicting the difference between 10-year pre-fire and 2-year post-fire values, with a median R^2 of 0.26 and 0.5, respectively. R² values for models predicting IE Regression were always low compared to other signatures. SE Regression also had relatively high R² values for models predicting 10-year pre-fire and 10-year post-fire signatures (median R^2 of 0.49 and 0.42, respectively). Post-fire models for IE Correlation and SE Correlation had very low R² values when predicting the difference between 10-year prefire signatures and 10- or 2-year post-fire signatures, but R² values were higher when predicting 10-year post-fire values (median R2 of

0.52 and 0.57, respectively). These results demonstrate that post-fire overland flow signatures (e.g. short or long-term post-fire signatures, changes in signatures with wildfire) can be predicted with sufficient performance.

We determined the most important variables for predicting signatures or changes in signatures with wildfire. The rankings of how many of the 100 ensemble RF models used each predictor in the modelling scenarios with the highest R² values (namely, predictions of 2-year post-fire IE Correlation and SE Correlation and the difference between pre-fire and 2-year post-fire IE Regression and SE Regression) are shown in Figure 6. The results for the average increase in MSE (IncMSE) when each predictor was permuted produced similar results for top predictors, therefore only the number of ensemble members using each predictor is presented here. Normalized difference vegetation index (NDVI) was in the top five predictors for each signature when predicting post-fire signature values, but not when predicting the change in signature values from pre-fire conditions. Average air temperature was a top predictor in the highest performing ensemble for each signature (10-year post-fire SE Correlation and IE Correlation and difference between 10-year pre-fire and 2-year post-fire IE Regression and SE Regression). Top predictors specific to IE Regression and SE Regression include the amount of developed/undeveloped land, basin and stream slope and soil layer thickness. Geologic strength, which is related to erodibility, was also frequently an important predictor for SE Regression. Clay content, soil saturated hydraulic conductivity and geologic permeability were important predictors in the models predicting post-fire SE Correlation and IE Correlation, which performed better than models predicting changes in these signatures with wildfire. The attributes related to fire (percent of the watershed burned and burn severity) were not of particularly high importance in any of the RF ensembles with high average R² values.

TABLE 2 Mean and median of the R^2 values for the 100 random forests run for the IE Regression, IE Correlation, SE Correlation, and SE Regression signatures.

	IE Regression	IE Correlation	SE Correlation	SE Regression		
10 years pre-fire						
Mean R ²	0.12	0.45	0.58	0.49		
Median R ²	0.12	0.45	0.59	0.49		
10 years pre-fire vs. 10 years post-fire						
Mean R ²	-0.02	-0.04	0.04	0.13		
Median R ²	-0.01	-0.04	0.06	0.12		
10 years post-fire						
Mean R ²	0.15	0.52	0.55	0.43		
Median R ²	0.18	0.52	0.57	0.42		
10 years pre-fire vs. 2 years post-fire						
Mean R ²	0.25	-0.04	-0.04	0.49		
Median R ²	0.26	-0.05	-0.06	0.50		
2 years post-fire						
Mean R ²	0.13	0.39	0.43	0.34		
Median R ²	0.15	0.46	0.52	0.35		

4 | DISCUSSION

The increases in IE Regression 2 years post-fire in the majority of sites align with previous observations of reduced soil infiltration capacity and reduced surface roughness after wildfire, all of which can contribute to flashier flow from increased surface runoff (Doerr et al., 2000; Ebel & Moody, 2016; Leighton-Boyce et al., 2007; Liu et al., 2021). These decreases in infiltration may also impact the ability of the soil profile to become saturated, which could explain the associated decrease in SE Regression and thus SE overland flow.

Studies of post-fire overland flow often focus on changes in infiltration in burned watersheds rather than saturation (e.g. Chen et al., 2013; DeBano, 2000; Ebel & Moody, 2017), though Holden et al. (2015) found that after prescribed fire in blanket peatlands, warmer soil temperatures and associated increased evapotranspiration led to deeper water tables. This reduced the prevalence of SE overland flow, especially shortly after burning. Scott and Van Wyk (1990) categorized overland flow occurring from hydrophobic layers below burn piles as SE. In post-fire soils with a shallow hydrophobic layer, the difference between IE and SE can become blurred. The hydrophobic layer can shorten the saturable depth of the soil profile, which would require less rainfall to produce SE overland flow. Conversely, the reduced infiltration capacity of hydrophobic soils (Ebel & Moody, 2017) could lend this phenomenon to being categorized as IE. In any case, the impacts of fire-induced hydrophobic soils on infiltration tend to be most prevalent during initial post-fire stages when the soil is the driest (DeBano, 2000), further supporting our finding that changes in overland flow were most pronounced 1-2 years after burning.

Our finding that IE overland flow signatures increase most in the first two years post-fire agrees with previous studies investigating the timescales of post-fire flooding and debris flows (Shakesby & Doerr, 2006; Stoof et al., 2012). The risk of post-fire hydrologic

hazards tends to decrease after two years as vegetation regrows and soils re-stabilize (Cannon et al., 2008; Kean et al., 2011; Rengers et al., 2020). Nevertheless, wildfires can have varying impacts on soil infiltration (DeBano & Krammes, 1966) and indeed there were watersheds in our study that experienced little-to-no change or experienced decreased values for IE-related signatures. In terms of runoff response to hydrophobic soils, DeBano and Krammes (1966) suggest that a degree of inherent hydrophobicity in soils makes further fire-induced hydrophobicity and associated decreases in infiltration more likely. A lack of inherent water repellency could explain small or non-existent increases in IE processes in some watersheds. This study demonstrates the utility of overland flow signatures for characterizing wildfire impacts on potential flood- or debris-flow-inducing surface runoff with relatively few parameters compared to modelling approaches. As future wildfires occur and streamflow is continuously measured at existing streamgages, signatures can be readily applied to understand the mechanisms of post-fire overland flow and assess hydrologic change and recovery.

The K-S tests suggest that pre- and post-fire distributions were mostly not statistically significantly different from each other regardless of the length of the post-fire period considered, except for comparisons between the pre-fire and 1 and 2-year post-fire SE Regression and 2-year post-fire IE Regression. The reason that IE Regression is more significantly affected after the second year post-fire, while SE Regression is impacted similarly for years 1 and 2, may be that short-term signatures (1- and 2-years post-fire) are calculated on a smaller number of events than longer-term signatures. It is thus possible that in a typical watershed from our dataset, there were insufficient events in the 1-year post-fire period with the precipitation intensity characteristics of high IE overland flow events to give significant values for the IE Regression signature. We ran the K-S tests with a sample size of 39 values for the pre- and post-fire period, but a larger sample size could aid in identifying changes with a wildfire that

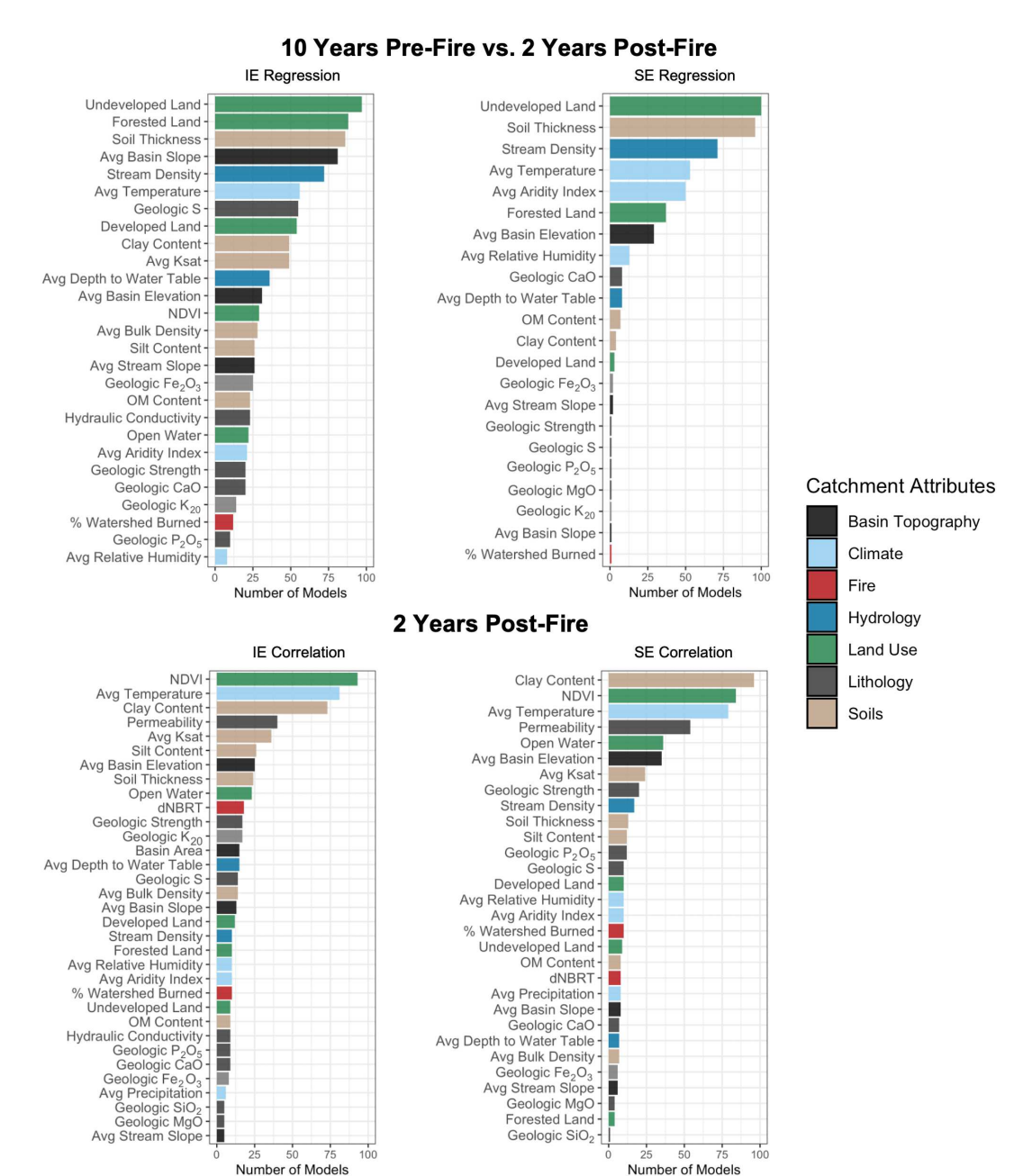


FIGURE 6 Bar plots representing the number of random forest models out of the 100 run for each signature in which each predictor variable was used. Predictors whose average increase in mean squared error (IncMSE) across the 100 random forest models was negative were excluded from plots and assumed to be relatively unimportant.

are more statistically significant. However, we showed that the post-fire shifts in overland flow in the study watersheds were hydrologically significant, by contextualizing pre- and post-fire signature values in the distribution of signature values from a large, diverse sample of U.S. watersheds calculated by McMillan et al. (2022) and Wu et al. (2021). In some cases, seemingly small changes in signature values with wildfire were associated with large changes in percentile in the distribution of signature values for catchments across the United States. This suggests that watersheds are hydrologically similar to very different watersheds in their post-fire period from the watersheds they were hydrologically similar to in their unburned condition. Understanding

these changes is crucial for adapting watershed management practices when faced with the potential risk of post-fire flooding or runoff-induced debris flows (Rengers et al., 2019).

4.1 | Comparison of hydrologic signatures

The signatures used in this study are based on regressions or correlations between event precipitation intensity or volume and streamflow statistics. Despite being designed for the same overland flow processes (IE Regression and IE Correlation for IE and SE Regression and SE

BOLOTIN and McMILLAN WILEY 13 of 18

Correlation for SE), the signatures designed by Wu et al. (2021) did not show changes in the post-fire period as clearly as the signatures from TOSSH. Wu et al. (2021) suggest that correlations between rainfall depth/intensity and runoff coefficient in IE Correlation and SE Correlation may be weaker than expected due to oversimplification of spatially variable rainfall by catchment-averaged rainfall values. We would expect this same issue to apply to the IE Regression and SE Regression signatures, though these generally produced a greater response for the same rainfall-runoff events. The regression producing the IE Regression and SE Regression signatures includes additional predictors of event precipitation volume or maximum intensity, such as antecedent precipitation and event average precipitation intensity (Estrany et al., 2010). These predictors potentially strengthen relationships with runoff response. The IE Regression and SE Regression signatures also regress predictors against both quickflow volume and peak flow, which may provide stronger relationships with event precipitation characteristics than runoff coefficient. McMillan et al. (2023) warn that signatures designed for particular climates may not function as expected in other climates and that the grid size of products like NLDAS-2 may result in inaccurate precipitation totals in small watersheds. Future investigation of why these signatures yield different results despite their similar regression-based methodologies is recommended.

Previous work suggests that the IE Regression and SE Regression signatures were designed for a semi-arid Mediterranean climate and may not function as expected in other climates McMillan et al. (2022). Approximately 1/4 of the watersheds studied receive >30% of annual precipitation as snow, which is not accounted for in the hydrologic signatures as implemented here, yet snowmelt as an antecedent moisture source can impact streamflow response at the event scale (Hammond & Kampf, 2020). Burned areas show impacts to snow accumulation and accelerated snowmelt after wildfire (Gleason et al., 2019; Kampf et al., 2022) and snowmelt can generate both saturation and IE as flowpaths converge within the snowpack (Webb et al., 2022). The missing representation of snowmelt could explain some of the variability in our signature values. In future work, incorporating the output from a snowmelt model in addition to event precipitation characteristics as signature inputs could help account for the role snowpack plays in determining surface water input, an approach that was used in a study of baseflow and storage signatures by (Wlostowski et al., 2021). The changes in values for the hydrologic signatures with wildfire aligned with our expectations. Nevertheless, it would be valuable to complement this study's large-sample approach with a small-sample, case study approach comparing signatures to field observations or model outputs of overland flow in burned watersheds in various climates, including those with significant snowfall. This would provide additional confidence that these signatures accurately represent overland flow processes.

4.2 | Regional patterns in signature changes

To identify regional patterns of signature changes, we mapped the short-term post-fire changes in signature values (Figure 7). The most

extreme changes in values for all signatures except IE Correlation occurred in the southwestern United States, with high increases in IE overland flow and decreases in SE overland flow in this region. The finding that most study sites experienced increased IE and decreased SE overland flow after wildfire according to hydrologic signatures could be biased by the high concentration of sites in this region.

Despite being geographically isolated from most of the study sites, watersheds in Florida and New Jersey did not show particularly distinct patterns, exhibiting relatively moderate changes in all signatures short-term after wildfire. Two of the watersheds located in Florida (Gage IDs 23 and 28, USGS-02330400 and USGS-02366996) experienced prescribed burns as opposed to wildfires, which typically burn at lower severities and are more spatially discontinuous than wildfires (Lucas-Borja et al., 2019). The signatures may reflect that these aspects of prescribed burning can reduce fire impacts on runoff generation by easing fire impacts on soil infiltration capacity, especially during low-intensity rainfall events (Lucas-Borja et al., 2019).

4.3 | Relevant predictors of post-fire signatures of overland flow

We show that climate, physiographic and wildfire attributes can predict post-fire hydrologic signatures of overland flow or changes to these signatures with burning. The distributions of signature values became less variable 10 years post-fire compared to the distributions 2 years post-fire, so it is reasonable that 10-year post-fire values were predicted more accurately than 2-year post-fire values. The SE Correlation and IE Correlation did not change as much as the IE Regression and SE Regression signatures (see Figure 2), which may explain the similar R^2 values for these signatures regardless of whether the preor post-fire values were predicted. With a larger training dataset, predictions of 2-year post-fire signatures or changes between 10-year pre-fire and 2-year post-fire signatures could be further improved. This would be a valuable contribution, given this is the post-fire period in which watershed managers most need to assess or predict the risk of post-fire hydrologic hazards.

Predictors related to wildfire (percent of the watershed burned and burn severity) in the RF models were not among the most used predictors for estimating post-fire signatures or changes in signatures with wildfire. These findings differ from Wilder et al. (2021) and Saxe et al. (2018), who both found the burned area to be an important predictor of post-fire hydrologic behaviour in RF regression models. Low correlations have been found between post-fire hydrologic response and predictor variables for watersheds with relatively small percentages of area burned (Saxe et al., 2018.) Our relatively high threshold of required burned area (30%) could have preemptively accounted for the importance of burned area for identifying a hydrologic response in burned watersheds, leading to low importance of this variable according to the RF models. Wildfire impacts on soil infiltration, which governs IE processes, are related to burn severity (Moody et al., 2016); however, results presented here and in Wilder et al. (2021) do not suggest that burn severity is a particularly important predictor of

Absolute Change in Signature Value 10 Years Pre-Fire to 2 Years Post-Fire

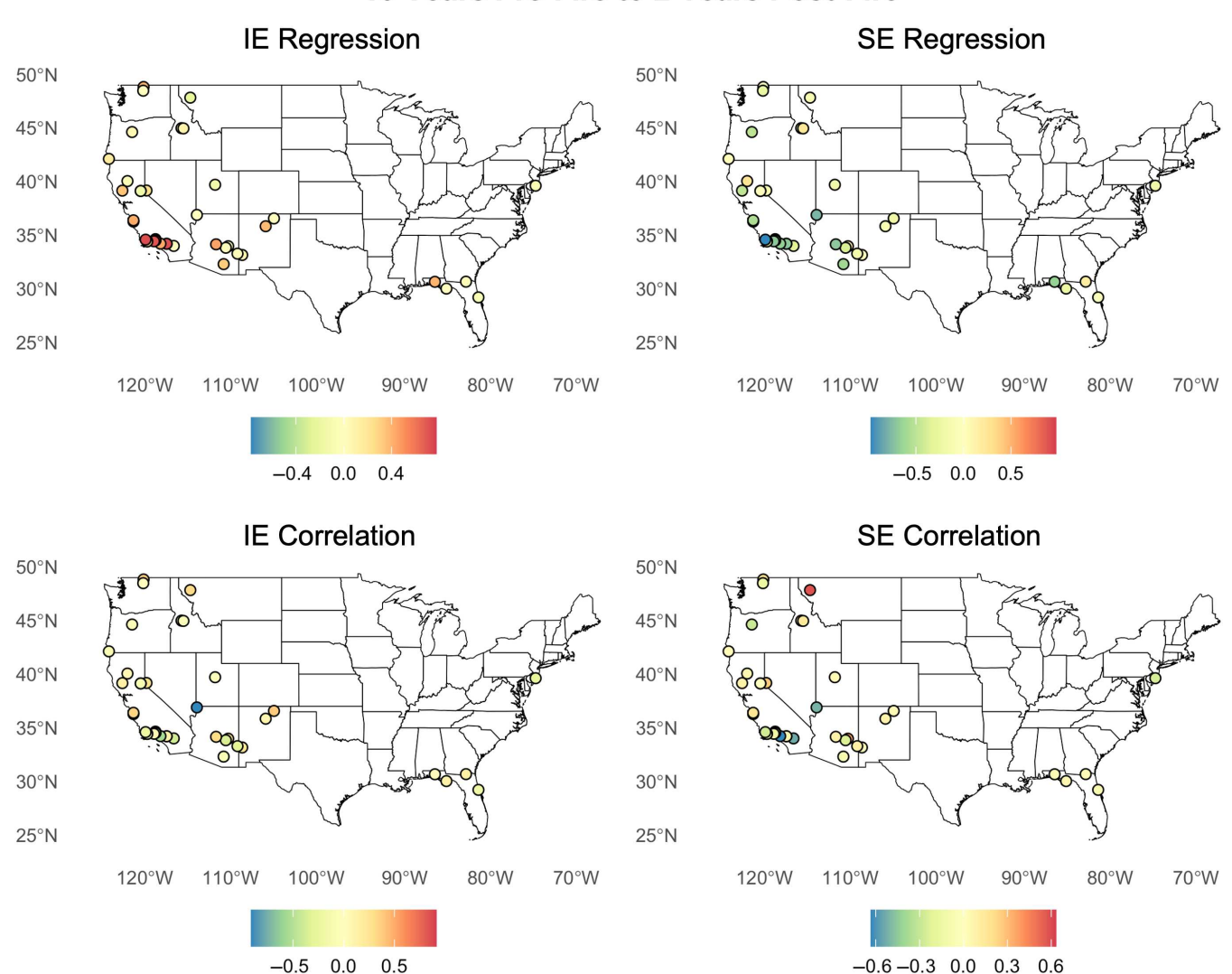


FIGURE 7 Maps of the absolute differences between 10-year pre-fire and 2-year post-fire signature values for the 39 study watersheds. Scales vary by signature, where blue represents larger decreases in signature value after wildfire and red represents larger increases in signature values after wildfire.

hydrologic response. This result may be sensitive to methodology when classifying burn severities. The most useful predictors of post-fire signatures or changes to signatures with wildfire, such as aridity index, NDVI, watershed slope and soil erodibility (geologic strength), echo previous findings related to overall streamflow response (Saxe et al., 2018).

NDVI quantifies photosynthetically active and transpiring vegetation and is related to canopy leaf area index (Cihlar et al., 1991). Vegetation intercepts water and stores and slows surface runoff by providing roughness in the litter layer (Leighton-Boyce et al., 2007). Therefore, it is reasonable that the pre-fire amount of photosynthesizing vegetation would be important for estimating overland flow. Calculation of a dynamic NDVI value quantifying loss of photosynthetically active vegetation with wildfire or short-term post-

fire NDVI was complicated by seasonal dynamics of this index due to plant phenology (Cihlar et al., 1991) and noise in the LANDSAT time series. This may explain why NDVI was not found to be an important predictor for *changes* in signatures with wildfire but was useful for predicting the pre-/post-fire values themselves. Average air temperature was included as a predictor in lieu of multiple correlated predictors generally related to climate. Climate influences vegetation and soil conditions that determine post-fire streamflow response (e.g. soil hydrophobicity, surface sealing and direct exposure to rainfall) (Hallema et al., 2017).

Maps of the catchment attributes most used by the best RF ensembles for each signature (see models included in Table 2) in Figure S3 show that the spatial variability in some of these attributes aligns with the spatial patterns of watersheds that experienced the

BOLOTIN and McMILLAN WII FY 15 of 18

greatest change in overland flow signatures with wildfire. In Figures S4-S8, we show scatter plots of the top three predictors in each RF model, against signature values for 10 years pre-fire, 2 and 10 years post-fire and signature change from 10 years pre-fire to 2 years post-fire or 10 years post-fire. Together, these results contextualize the directionality of relationships between the catchment attributes and post-fire signatures or signature changes with wildfire from the RF analysis. For example, stream density is relatively high in southwestern watersheds where IE Regression exhibited the greatest increases and SE Regression exhibited the greatest decreases two years post-fire. Overland flow can quickly develop in small, steep watersheds with high drainage densities (Baker, 1977), making these watersheds more reactive to precipitation amount and intensity in a post-fire context (Cannon et al., 2008). Several of the variables we found to be most useful for predicting post-fire overland flow signatures agree with the literature, yet the robustness of these conclusions would benefit from future work determining the most reliable overland flow signatures for a post-fire context.

5 | CONCLUSIONS

We demonstrated the utility of hydrologic signatures of overland flow for investigating post-fire overland flow processes. Some signatures showed increased IE processes and decreased SE processes after wildfire, especially in the first 2 years post-fire, for 56% and 82% of the 39 watersheds in this study, respectively. These increases in IE processes may make watersheds vulnerable to runoff-induced postfire debris flows that threaten humans, water quality and infrastructure. However, there was some disagreement among signatures that theoretically represent the same process and further work to identify robust signatures of overland flow for investigating post-fire processes is recommended. While changes in signatures with wildfire were not statistically significant across all watersheds, they were hydrologically significant compared to signature values from a large national sample of watersheds. We demonstrate that post-fire signatures of overland flow or changes in these signatures from pre-fire conditions after burning can be predicted sufficiently using attributes related to watersheds, climate and wildfires. IE Regression was the hardest signature to predict. NDVI, air temperature, amount of developed/undeveloped land and soil thickness and clay content were the most used predictors by well-performing RF models. The mean and median R² values were highest for RF ensembles predicting shortterm change in IE Regression and SE Regression with wildfire or predicting long-term post-fire IE Correlation and SE Correlation.

Watersheds in this study were highly concentrated in the arid and semi-arid southwestern United States. Consequently, future work to build a larger, more diverse training dataset of burned watersheds and their attributes for ML models predicting signatures is recommended. This will promote differentiation between regionally specific versus widespread patterns in post-fire signatures of overland flow. Given the high occurrence of large wildfires in the western United States in recent years (Goss et al., 2020; Keeley & Syphard, 2021), future

studies may further advance efforts to predict changes in overland flow signatures with wildfire with additional data. Improving these predictions would aid watershed managers in post-fire flooding and debris-flow hazard mitigation by further elucidating the drivers and temporal dynamics of post-fire overland flow.

Signatures of overland flow provide a relatively streamlined method for assessing and monitoring wildfire impacts on overland flow, which can benefit rapid post-fire hydrologic hazard assessment and response planning. The results and methodology presented here demonstrate the utility of hydrologic signatures for improving a generalized understanding of post-fire overland flow processes with potential application to prediction in ungauged or recently burned basins.

ACKNOWLEDGEMENTS

This material is based upon work supported by the National Science Foundation under Grant No. 2124923. We thank Dr. Trent Biggs and Dr. Alicia Kinoshita for their feedback on the text and methods, Dr. Dan Sousa for advice on remote sensing methods, Mallorie Honey and Margot Mattson for help obtaining satellite imagery and Donny Kim for help obtaining precipitation data.

DATA AVAILABILITY STATEMENT

Data produced and used in this study is publicly available, aside from that which was obtained directly from the authors of other studies or from publicly available resources (see Table 2). Files containing the results of this study are available at 10.5281/zenodo.10607977.

ORCID

L. A. Bolotin https://orcid.org/0000-0002-0295-9544

REFERENCES

Abatzoglou, J. T., & Williams, A. P. (2016). Impact of anthropogenic climate change on wildfire across western US forests. *Proceedings of the National Academy of Sciences*, 113(42), 11770–11775. https://doi.org/10.1073/pnas.1607171113

Addor, N., Nearing, G., Prieto, C., Newman, A. J., Le Vine, N., & Clark, M. P. (2018). A ranking of hydrological signatures based on their predictability in space. Water Resources Research, 54(11), 8792–8812. https://doi.org/10.1029/2018WR022606

Addor, N., Newman, A. J., Mizukami, N., & Clark, M. P. (2017). The CAMELS data set: Catchment attributes and meteorology for largesample studies. *Hydrology and Earth System Sciences*, 21(10), 5293– 5313.

AghaKouchak, A., Chiang, F., Huning, L. S., Love, C. A., Mallakpour, I., Mazdiyasni, O., Moftakhari, H., Papalexiou, S. M., Ragno, E., & Sadegh, M. (2020). Climate extremes and compound hazards in a warming world. *Annual Review of Earth and Planetary Sciences*, 48(1), 519–548. https://doi.org/10.1146/annurev-earth-071719-055228

Baker, V. R. (1977). Stream-channel response to floods, with examples from central Texas. *Geological Society of America Bulletin*, 88(8), 1057. https://doi.org/10.1130/0016-7606(1977)88<1057:SRTFWE>2.0.CO;2

Basso, M., Vieira, D. C. S., Ramos, T. B., & Mateus, M. (2020). Assessing the adequacy of SWAT model to simulate postfire effects on the watershed hydrological regime and water quality. *Land Degradation & Development*, 31(5), 619–631. https://doi.org/10.1002/ldr.3476



- Beck, H. E., De Roo, A., & Van Dijk, A. I. J. M. (2015). Global maps of streamflow characteristics based on observations from several thousand catchments. *Journal of Hydrometeorology*, 16(4), 1478–1501. https://doi.org/10.1175/JHM-D-14-0155.1
- Beven, K. J. (2020). A history of the concept of time of concentration. Hydrology and Earth System Sciences, 24(5), 2655–2670. https://doi.org/10.5194/hess-24-2655-2020
- Buchanan, B., Auerbach, D. A., Knighton, J., Evensen, D., Fuka, D. R., Easton, Z., Wieczorek, M., Archibald, J. A., McWilliams, B., & Walter, T. (2018). Estimating dominant runoff modes across the conterminous United States. *Hydrological Processes*, 32(26), 3881–3890. https://doi.org/10.1002/hyp.13296
- Cannon, S. H., Gartner, J. E., Wilson, R. C., Bowers, J. C., & Laber, J. L. (2008). Storm rainfall conditions for floods and debris flows from recently burned areas in southwestern Colorado and southern California. *Geomorphology*, 96(3-4), 250-269. https://doi.org/10.1016/j.geomorph.2007.03.019
- Chen, L., Berli, M., & Chief, K. (2013). examining modeling approaches for the rainfall-runoff process in wildfire-affected watersheds: Using san dimas experimental forest. JAWRA Journal of the American Water Resources Association, 49(4), 851–866. https://doi.org/10.1111/jawr. 12043
- Cihlar, J., Laurent, L. S., & Dyer, J. A. (1991). Relation between the normalized difference vegetation index and ecological variables. *Remote Sensing of Environment*, 35(2–3), 279–298. https://doi.org/10.1016/0034-4257(91)90018-2
- David, P. C., Chaffe, P. L. B., Chagas, V. B. P., Dal Molin, M., Oliveira, D. Y., Klein, A. H. F., & Fenicia, F. (2022). Correspondence between model structures and hydrological signatures: A large-sample case study using 508 Brazilian catchments. Water Resources Research, 58(3), e2021WR030619. https://doi.org/10.1029/2021WR030619
- De Cicco, L. A., Hirsch, R. M., Lorenz, D., Watkins, D., & Johnson, M. (2018). DataRetrieval [Computer software]. U.S. Geological Survey. https://doi.org/10.5066/P9X4L3GE
- DeBano, L. F. (2000). The role of fire and soil heating on water repellency in wildland environments: A review. *Journal of Hydrology*, 231–232, 195–206. https://doi.org/10.1016/S0022-1694(00)00194-3
- DeBano, L. F., & Krammes, J. S. (1966). Water repellent soils and their relation to wildfire temperatures. *International Association of Scientific Hydrology*. *Bulletin*, 11(2), 14–19. https://doi.org/10.1080/02626666609493457
- Dick, G. S., Anderson, R. S., & Sampson, D. E. (1997). Controls on flash flood magnitude and hydrograph shape, Upper Blue Hills badlands, Utah. *Geology*, 25(1), 45. https://doi.org/10.1130/0091-7613(1997) 025<0045:COFFMA>2.3.CO;2
- Doerr, S. H., Shakesby, R. A., & Walsh, R. P. D. (2000). Soil water repellency: Its causes, characteristics and hydro-geomorphological significance. *Earth-Science Reviews*, 51(1–4), 33–65. https://doi.org/10.1016/S0012-8252(00)00011-8
- Dunne, T., & Black, R. D. (1970). Partial area contributions to storm runoff in a small new england watershed. Water Resources Research, 6(5), 1296–1311. https://doi.org/10.1029/WR006i005p01296
- Ebel, B. A., & Moody, J. A. (2017). Synthesis of soil-hydraulic properties and infiltration timescales in wildfire-affected soils: Synthesis of soil-hydraulic properties in wildfire-affected soils. Hydrological Processes, 31(2), 324–340. https://doi.org/10.1002/hyp.10998
- Eidenshink, J., Schwind, B., Brewer, K., Zhu, Z.-L., Quayle, B., & Howard, S. (2007). A project for monitoring trends in burn severity. *Fire Ecology*, 3(1), 3–21. https://doi.org/10.4996/fireecology.0301003
- Estrany, J., Garcia, C., & Batalla, R. J. (2010). Hydrological response of a small mediterranean agricultural catchment. *Journal of Hydrology*, 380(1–2), 180–190. https://doi.org/10.1016/j.jhydrol. 2009.10.035

- Falcone, J. A. (2011). GAGES-II: Geospatial attributes of gages for evaluating streamflow, USGS Publications Warehouse. https://doi.org/10.3133/70046617
- Gleason, K. E., McConnell, J. R., Arienzo, M. M., Chellman, N., & Calvin, W. M. (2019). Four-fold increase in solar forcing on snow in western U.S. burned forests since 1999. *Nature Communications*, 10(1), 2026. https://doi.org/10.1038/s41467-019-09935-v
- Gnann, S. J., Coxon, G., Woods, R. A., Howden, N. J. K., & McMillan, H. K. (2021). TOSSH: A toolbox for streamflow signatures in hydrology. Environmental Modelling & Software, 138, 104983. https://doi.org/10. 1016/j.envsoft.2021.104983
- Goss, M., Swain, D. L., Abatzoglou, J. T., Sarhadi, A., Kolden, C. A., Williams, A. P., & Diffenbaugh, N. S. (2020). Climate change is increasing the likelihood of extreme autumn wildfire conditions across California. *Environmental Research Letters*, 15(9), 094016. https://doi.org/ 10.1088/1748-9326/ab83a7
- Gupta, H. V., Perrin, C., Blöschl, G., Montanari, A., Kumar, R., Clark, M., & Andréassian, V. (2014). Large-sample hydrology: A need to balance depth with breadth. *Hydrology and Earth System Sciences*, 18(2), 463–477. https://doi.org/10.5194/hess-18-463-2014
- Gupta, H. V., Wagener, T., & Liu, Y. (2008). Reconciling theory with observations: Elements of a diagnostic approach to model evaluation. Hydrological Processes, 22(18), 3802–3813. https://doi.org/10.1002/hyp.6989
- Hallema, D. W., Sun, G., Bladon, K. D., Norman, S. P., Caldwell, P. V., Liu, Y., & McNulty, S. G. (2017). Regional patterns of postwildfire streamflow response in the Western United States: The importance of scale-specific connectivity. *Hydrological Processes*, 31(14), 2582–2598. https://doi.org/10.1002/hyp.11208
- Hammond, J. C., & Kampf, S. K. (2020). Subannual streamflow responses to rainfall and snowmelt inputs in snow-dominated watersheds of the Western United States. Water Resources Research, 56(4), e2019WR026132. https://doi.org/10.1029/2019WR026132
- Hampton, T. B., & Basu, N. B. (2022). A novel Budyko-based approach to quantify post-forest-fire streamflow response and recovery timescales. *Journal of Hydrology*, 608, 127685. https://doi.org/10.1016/j. jhydrol.2022.127685
- Holden, J., Palmer, S. M., Johnston, K., Wearing, C., Irvine, B., & Brown, L. E. (2015). Impact of prescribed burning on blanket peat hydrology. Water Resources Research, 51(8), 6472–6484. https://doi.org/10.1002/2014WR016782
- Horton, R. E. (1933). The Rôle of infiltration in the hydrologic cycle. *Transactions of the American Geophysical Union*, 14(1), 446–460. https://doi.org/10.1029/TR014i001p00446
- Jehn, F. U., Bestian, K., Breuer, L., Kraft, P., & Houska, T. (2020). Using hydrological and climatic catchment clusters to explore drivers of catchment behavior. *Hydrology and Earth System Sciences*, 24(3), 1081–1100. https://doi.org/10.5194/hess-24-1081-2020
- Kampf, S. K., McGrath, D., Sears, M. G., Fassnacht, S. R., Kiewiet, L., & Hammond, J. C. (2022). Increasing wildfire impacts on snowpack in the western US. Proceedings of the National Academy of Sciences, 119(39), e2200333119.
- Kean, J. W., & Staley, D. M. (2021). Forecasting the frequency and magnitude of postfire debris flows across Southern California. Earth's Future, 9(3), e2020EF001735. https://doi.org/10.1029/2020EF001735
- Kean, J. W., Staley, D. M., & Cannon, S. H. (2011). In situ measurements of post-fire debris flows in southern California: Comparisons of the timing and magnitude of 24 debris-flow events with rainfall and soil moisture conditions. *Journal of Geophysical Research*, 116(F4), F04019. https://doi.org/10.1029/2011JF002005
- Kean, J. W., Staley, D. M., Lancaster, J. T., Rengers, F. K., Swanson, B. J., Coe, J. A., Hernandez, J. L., Sigman, A. J., Allstadt, K. E., &

BOLOTIN and McMILLAN WILEY 17 of 18

- Lindsay, D. N. (2019). Inundation, flow dynamics, and damage in the 9 January 2018 Montecito debris-flow event, California, USA: Opportunities and challenges for post-wildfire risk assessment. *Geosphere*, 15(4), 1140–1163. https://doi.org/10.1130/GES02048.1
- Keeley, J. E., & Syphard, A. D. (2021). Large California wildfires: 2020 fires in historical context. Fire Ecology, 17(1), 22. https://doi.org/10.1186/ s42408-021-00110-7
- Kuhn, M. (2008). Building predictive models in R using the caret package. Journal of Statistical Software, 28(5), 1–26. https://doi.org/10.18637/ iss.v028.i05
- Leighton-Boyce, G., Doerr, S. H., Shakesby, R. A., & Walsh, R. P. D. (2007). Quantifying the impact of soil water repellency on overland flow generation and erosion: A new approach using rainfall simulation and wetting agent onin situ soil. *Hydrological Processes*, 21(17), 2337–2345. https://doi.org/10.1002/hyp.6744
- Liaw, A., & Wiener, M. (2002). Classification and Regression by random-Forest. R News, 2(3), 18–22.
- Liu, T., McGuire, L. A., Wei, H., Rengers, F. K., Gupta, H., Ji, L., & Goodrich, D. C. (2021). The timing and magnitude of changes to Hortonian overland flow at the watershed scale during the post-fire recovery process. *Hydrological Processes*, 35(5), e14208. https://doi.org/10.1002/hyp.14208
- Lucas-Borja, M. E., Plaza-Álvarez, P. A., Gonzalez-Romero, J., Sagra, J., Alfaro-Sánchez, R., Zema, D. A., Moya, D., & De Las Heras, J. (2019). Short-term effects of prescribed burning in Mediterranean pine plantations on surface runoff, soil erosion and water quality of runoff. Science of the Total Environment, 674, 615–622. https://doi.org/10.1016/j.scitotenv.2019.04.114
- McMillan, H. (2020). Linking hydrologic signatures to hydrologic processes: A review. *Hydrological Processes*, 34(6), 1393–1409. https://doi.org/10.1002/hyp.13632
- McMillan, H., Coxon, G., Araki, R., Salwey, S., Kelleher, C., Zheng, Y., Knoben, W., Gnann, S., Seibert, J., & Bolotin, L. (2023). When good signatures go bad: Applying hydrologic signatures in large sample studies. Hydrological Processes, 37(9), e14987. https://doi.org/10.1002/hyp. 14987
- McMillan, H. K. (2021). A review of hydrologic signatures and their applications. WIREs Water, 8(1), e1499. https://doi.org/10.1002/wat2.1499
- McMillan, H. K., Gnann, S. J., & Araki, R. (2022). Large scale evaluation of relationships between hydrologic signatures and processes. Water Resources Research, 58(6), e2021WR031751. https://doi.org/10. 1029/2021WR031751
- Moody, J. A., Ebel, B. A., Nyman, P., Martin, D. A., Stoof, C., & McKinley, R. (2016). Relations between soil hydraulic properties and burn severity. International Journal of Wildland Fire, 25(3), 279. https://doi.org/10.1071/WF14062
- Newman, A. J., Clark, M. P., Sampson, K., Wood, A., Hay, L. E., Bock, A., Viger, R. J., Blodgett, D., Brekke, L., Arnold, J. R., Hopson, T., & Duan, Q. (2015). Development of a large-sample watershed-scale hydrometeorological data set for the contiguous USA: Data set characteristics and assessment of regional variability in hydrologic model performance. Hydrology and Earth System Sciences, 19(1), 209–223. https://doi.org/10.5194/hess-19-209-2015
- Rengers, F. K., McGuire, L. A., Kean, J. W., Staley, D. M., & Youberg, A. M. (2019). Progress in simplifying hydrologic model parameterization for broad applications to post-wildfire flooding and debris-flow hazards. *Earth Surface Processes and Landforms*, 44(15), 3078–3092. https://doi.org/10.1002/esp.4697
- Rengers, F. K., McGuire, L. A., Oakley, N. S., Kean, J. W., Staley, D. M., & Tang, H. (2020). Landslides after wildfire: Initiation, magnitude, and mobility. *Landslides*, 17(11), 2631–2641. https://doi.org/10.1007/s10346-020-01506-3

- Robinson, J. S., Sivapalan, M., & Snell, J. D. (1995). On the relative roles of hillslope processes, channel routing, and network geomorphology in the hydrologic response of natural catchments. Water Resources Research, 31(12), 3089–3101. https://doi.org/10.1029/ 95WR01948
- Saxe, S., Hogue, T. S., & Hay, L. (2018). Characterization and evaluation of controls on post-fire streamflow response across western US watersheds. *Hydrology and Earth System Sciences*, 22(2), 1221–1237. https://doi.org/10.5194/hess-22-1221-2018
- Scott, D. F., & Van Wyk, D. B. (1990). The effects of wildfire on soil wettability and hydrological behaviour of an afforested catchment. *Journal* of Hydrology, 121(1-4), 239-256. https://doi.org/10.1016/0022-1694(90)90234-O
- Shafii, M., & Tolson, B. A. (2015). Optimizing hydrological consistency by incorporating hydrological signatures into model calibration objectives: Hydrological consistency optimization. Water Resources Research, 51(5), 3796-3814. https://doi.org/10.1002/2014WR01 6520
- Shakesby, R., & Doerr, S. (2006). Wildfire as a hydrological and geomorphological agent. *Earth-Science Reviews*, 74(3-4), 269-307. https://doi.org/10.1016/j.earscirev.2005.10.006
- Stoof, C. R., Vervoort, R. W., Iwema, J., Van Den Elsen, E., Ferreira, A. J. D., & Ritsema, C. J. (2012). Hydrological response of a small catchment burned by experimental fire. *Hydrology and Earth System Sciences*, 16(2), 267–285. https://doi.org/10.5194/hess-16-267-2012
- Tomkins, K. M., Humphreys, G. S., Gero, A. F., Shakesby, R. A., Doerr, S. H., Wallbrink, P. J., & Blake, W. H. (2008). Postwildfire hydrological response in an El Niño–Southern Oscillation–dominated environment. *Journal of Geophysical Research*, 113(F2), F02023. https://doi.org/10. 1029/2007JF000853
- Wagenbrenner, J. W., Ebel, B. A., Bladon, K. D., & Kinoshita, A. M. (2021). Post-wildfire hydrologic recovery in Mediterranean climates: A systematic review and case study to identify current knowledge and opportunities. *Journal of Hydrology*, 602, 126772. https://doi.org/10.1016/j.jhydrol.2021.126772
- Wall, S. A., Roering, J. J., & Rengers, F. K. (2020). Runoff-initiated post-fire debris flow Western Cascades, Oregon. *Landslides*, 17(7), 1649–1661. https://doi.org/10.1007/s10346-020-01376-9
- Webb, R. W., Musselman, K. N., Ciafone, S., Hale, K. E., & Molotch, N. P. (2022). Extending the vadose zone: Characterizing the role of snow for liquid water storage and transmission in streamflow generation. Hydrological Processes, 36(3), e14541. https://doi.org/10.1002/hyp. 14541
- Wieczorek, M. E., Jackson, S. E., & Schwarz, G. E. (2018). Select Attributes for NHDPlus Version 2.1 Reach Catchments and Modified Network Routed Upstream Watersheds for the Conterminous United States [Data set]. U.S. Geological Survey. https://doi.org/ 10.5066/F7765D7V
- Wilder, B. A., Lancaster, J. T., Cafferata, P. H., Coe, D. B. R., Swanson, B. J., Lindsay, D. N., Short, W. R., & Kinoshita, A. M. (2021). An analytical solution for rapidly predicting post-fire peak streamflow for small watersheds in southern California. *Hydrological Processes*, 35(1), e13976. https://doi.org/10.1002/hyp.13976
- Wlostowski, A. N., Molotch, N., Anderson, S. P., Brantley, S. L., Chorover, J., Dralle, D., Kumar, P., Li, L., Lohse, K. A., Mallard, J. M., McIntosh, J. C., Murphy, S. F., Parrish, E., Safeeq, M., Seyfried, M., Shi, Y., & Harman, C. (2021). Signatures of hydrologic function across the critical zone observatory network. Water Resources Research, 57(3), e2019WR026635. https://doi.org/10.1029/2019 WR026635
- Wu, S., Zhao, J., Wang, H., & Sivapalan, M. (2021). Regional patterns and physical controls of streamflow generation across the conterminous

- United States. Water Resources Research, 57(6), e2020WR028086. https://doi.org/10.1029/2020WR028086
- Xia, Y., Mitchell, K., Ek, M., Cosgrove, B., Sheffield, J., Luo, L., Alonge, C., Wei, H., Meng, J., Livneh, B., Duan, Q., & Lohmann, D. (2012). Continental-scale water and energy flux analysis and validation for North American Land Data Assimilation System project phase 2 (NLDAS-2): 2. Validation of model-simulated streamflow. *Journal of Geophysical Research: Atmospheres*, 117(D3), D03109. https://doi.org/10.1029/2011JD016051
- Yin, J., Gentine, P., Zhou, S., Sullivan, S. C., Wang, R., Zhang, Y., & Guo, S. (2018). Large increase in global storm runoff extremes driven by climate and anthropogenic changes. *Nature Communications*, 9(1), 4389. https://doi.org/10.1038/s41467-018-06765-2

SUPPORTING INFORMATION

Additional supporting information can be found online in the Supporting Information section at the end of this article.

How to cite this article: Bolotin, L. A., & McMillan, H. (2024). A hydrologic signature approach to analysing wildfire impacts on overland flow. *Hydrological Processes*, 38(6), e15215. https://doi.org/10.1002/hyp.15215